Energy Demand Analysis for eVTOL Charging Stations in Urban Air Mobility

Abenezer Taye* and Peng Wei†
The George Washington University, Washington, D.C. 20052, USA

Priyank Pradeep‡
Universities Space Research Association, Washington, DC 20024

James Jones§, Timothy Bonin¶, and Derek Eberle ‖
MIT Lincoln Laboratory, Lexington, MA 02421, USA

Electric-powered aircraft, commonly known as eVTOLs (electric vertical takeoff and landing aircraft), are expected to enable urban air mobility (UAM) operations. A critical factor for the successful deployment of UAM with eVTOLs is understanding the electrical energy demand at their charging stations. This paper introduces a methodology based on an energy consumption model for eVTOLs to determine the charging requirements for UAM operations. We apply this method to a case study in a large UAM network within the Dallas-Fort Worth (DFW) area, using a 4-hour operational time horizon. Our approach to forecasting charging demand incorporates key factors that significantly influence energy consumption in UAM, such as aircraft models, wind forecasts, and a detailed list of flight missions over the specified forecast period. Additionally, we have integrated the charging process with the demand forecasting process to ensure an accurate estimation of the aggregated power demand at each vertiport during the forecasting time horizon. The results of our study demonstrate that the charging demand at a vertiport is primarily affected by the number of departing flight missions and their departure schedules. The insights gained from this study are essential for planning and developing efficient charging infrastructure, thereby ensuring the sustainable implementation of eVTOLs in urban environments.

I. Nomenclature

x_t	=	State of the aircraft at time t
u_t	=	Control input of the aircraft at time t
λ	=	Latitude
τ	=	Longitude
V	=	True airspeed
ψ	=	Heading angle w.r.t. north
T	=	Net thrust
θ	=	Rotor tip-path-plane pitch angle
ϕ	=	Rotor tip-path-plane roll (bank) angle
D	=	Parasite drag
m	=	Mass of the aircraft
R_{earth}	=	Radius of the Earth
h	=	Altitude of aircraft above mean sea level
A_{rotor}	=	Rotor area

*Graduate Research Assistant, Mechanical and Aerospace Engineering Department, School of Engineering and Applied Science, AIAA Member.
†Assistant Professor, Mechanical and Aerospace Engineering Department, School of Engineering and Applied Science, AIAA Senior Member.
‡Senior Aerospace Engineer, Universities Space Research Association, AIAA Senior Member
§Technical Staff, Air Traffic Control Systems Group, AIAA Senior Member
¶Technical Staff, Air Traffic Control Systems Group
‖Technical Staff, Air Traffic Control Systems Group

σ	=	Thrust-to-weight solidity ratio
C_d	=	Mean blade drag coefficient
F_i	=	Feasibility of flight mission i
F_P	=	Function accounting for blade section velocity increase
P_{required}	=	Required power
P_{induced}	=	Induced power
P_{parasite}	=	Parasite power
P_{profile}	=	Profile power
κ	=	Induced power correction factor
v_i	=	Induced velocity
α	=	Angle of attack
Ω	=	Rotational velocity of the rotor blades
E_{consumed}	=	Energy consumed by a flight
E_{battery}	=	Battery capacity
P_{charging}	=	Charging power of eVTOL charger
γ	=	Slope of the line for charging power
$E_{\text{full charge}}$	=	Energy needed to fully charge the battery
eVTOL	=	Electric Vertical Take Off and Landing vehicle
SoC	=	State of Charge
UAM	=	Urban Air Mobility
DFW	=	Dallas-Fort Worth
WRF	=	Weather Research and Forecasting

II. Introduction

A. Motivation

Urban Air Mobility (UAM) is a novel concept in which partially or fully autonomous air vehicles transport passengers and cargo in dense urban environments. This technology aims to provide a safe, efficient, and accessible on-demand air transportation system [1], offering an alternative to traditional ground-based transportation methods. Furthermore, as the technology advances, it will connect urban centers to suburban areas, expanding the reach of metropolitan regions.

Electric-powered aircraft, denominated eVTOLs (electric vertical takeoff and landing aircraft), are expected to enable UAM operations. Several companies such as Airbus A^3, Aurora Flight Sciences, EHang, Joby Aviation, Kitty Hawk, Leonardo, Lilium, and Volvocopter, have introduced a variety of eVTOL designs. However, one thing all these designs have in common is they are all powered by electricity. Therefore, one of the important aspects of the successful implementation of UAM using eVTOLs is the study of electrical energy demand at the charging stations for these electric aircraft.

Accurate forecasting of energy demand at charging stations is a crucial and challenging task. Studies have shown that failing to accurately predict the load at these stations can lead to significant adverse effects on the safety and efficiency of existing power systems. These include unstable voltage and frequency, substantial harmonic injection, increased power losses, and overall instability of the power system [2]. This study introduces a method for analyzing and forecasting the energy demand at vertiports, aiming to support UAM operations over a specified period.

B. Related Work

In the literature, the issue of load forecasting at charging stations for electric vehicles (EVs), particularly in the context of the broader electrification of mobility, has been extensively explored. These methodologies are generally categorized into two types: model-based and data-driven techniques. The model-based approaches to load forecasting primarily employ mathematical models to predict expected load profiles. Within this category, the most common methods in the EV sector include the state-of-charge (SoC) model [3], the energy consumption model [4], and the Monte Carlo simulations method [5].

On the other hand, data-driven techniques leverage historical charging patterns combined with machine learning models to forecast expected loads at charging stations. In this domain, Liao et al. [6] developed a technique based on Support Vector Machine (SVM) for charging load forecasting, while Sun et al. [7] employed Support Vector Regression

(SVR). Additionally, Dabbaghjamanesh et al. [8] introduced a Q-learning-based approach for this purpose. Although these methods effectively forecast charging demands at stations, they are primarily designed for electric ground vehicles.

In the context of UAM operations, [9] studied the impact of UAM operations on the national power grid. Moreover, [10] addressed the problem of eVTOL fleet dispatching while considering the charging costs at the vertiports. However, both studies assumed a uniform energy consumption rate across all UAM operations, neglecting to account for various scenario-specific and mission-specific factors that influence the energy use in UAM operations.

According to Park [11], three primary factors are identified as influencing load profiles: the location of charging, the charging need, and the timing of charging. This research assumes that charging will occur at vertiports, the designated take-off points for the aircraft. Furthermore, it is presumed that each aircraft will be fully charged prior to take-off, positioning the charging time immediately before each mission. However, determining the charging need, which is defined as the electric energy used by the aircraft during flight and, therefore transferred from the grid to the battery when charging, requires a detailed investigation for each specific mission in a scenario. Therefore, the main focus of this research is to develop a methodology for determining the charging needs of UAM operations.

C. Contribution of this Paper

The main contribution of this paper is the development of a methodology for estimating the charging needs at vertiports, which takes into account significant factors affecting the energy consumption of each flight mission, including flight plans, wind conditions, and the aircraft energy consumption model. Additionally, we have integrated aircraft scheduling and the charging process into the charging demand forecasting procedure to accurately estimate the charging demand at the vertiport for a given time horizon.

III. Problem Formulation

In this paper, we consider structured airspace where predefined routes, vertiport locations, the number of eVTOLs, the wind forecast, and the flight schedules are known. Our aim is to forecast the energy demand at charging stations for a specified time period. To achieve this, we utilize an energy consumption model approach. This involves calculating the energy consumption for each mission within the designated time frame using the aircraft energy consumption model. Finally, the sum of these individual mission-specific energy consumption represents the total energy demand at the charging stations. In the remaining part of this section, we outline the background materials required to understand the power consumption model formulation. First, a point mass guidance model of eVTOL aircraft presented in [12] is introduced. Then, the power consumption model that is used to compute the mission-level energy requirement of the aircraft is presented.

A. Aircraft Model

The eVTOL aircraft lateral flight dynamics model, shortly described by the differential equation:

$$\dot{x}_t = \xi(x_t, u_t) \tag{1}$$

operates within two-dimensional space. In this model, $x_t \in \mathbb{R}^2$ and $u_t \in \mathbb{R}^3$ represent the state and control input of the aircraft at time t, respectively. This model can capture the cruise phase of the flight mission. The states of the model are $x = [\lambda, \tau, s, \psi]$, where λ is the latitude, τ is the longitude, V is the true airspeed, and ψ is the heading angle w.r.t. north. The control inputs of the model are the net thrust (T), the rotor tip-path-plane pitch angle (θ), and the rotor tip-path-plane roll (bank) angle (ϕ).

$$\frac{dV}{dt} = \frac{T\cos\phi\sin\theta - D}{m} \tag{2}$$

$$V\frac{d\psi}{dt} = \frac{T\sin\phi}{m} \tag{3}$$

$$(R_{\text{earth}} + h)\frac{d\lambda}{dt} = V\cos\psi \tag{4}$$

$$(R_{\text{earth}} + h)\cos\lambda\frac{d\tau}{dt} = V\sin\psi \tag{5}$$

The multi-rotor aircraft is assumed to have four rotors and the net thrust (T) generated by the aircraft is a sum of thrusts generated by each motor (T_{rotor}). Therefore, $T = 4T_{\text{rotor}}$, and parasite drag (D) on the multi-rotor eVTOL is calculated as $D = 1.1984\frac{\rho V^2}{2}$, where ρ is the density of air [13].

B. Power Consumption Model

The power consumption model we implement to compute the mission-level energy requirement is based on momentum theory for rotorcraft and is adopted from [12] and [14]. In the following, we summarize the main components of the power consumption model. Assuming a quasi-steady flight, the instantaneous power required for forward cruise flight at a constant altitude is given by the sum of induced power, parasite power, and profile power:

$$P_{\text{required}} = P_{\text{induced}} + P_{\text{parasite}} + P_{\text{profile}} \tag{6}$$

The induced power (P_{induced}) is equal to the sum of the induced power losses of each rotor ($P_{\text{induced rotor}}$). Therefore, P_{induced} is given as:

$$P_{\text{induced}} = \sum_{n=1}^{4}(P_{\text{induced rotor}})_n = \kappa \sum_{n=1}^{4}(T_{\text{rotor}})_n(v_i)_n, \tag{7}$$

where κ is the induced power correction factor and v_i is the induced velocity. The parasite power loss (P_{parasite}), which is the power to propel the aircraft forward at a constant altitude is given by:

$$P_{\text{parasite}} = TV \sin\alpha, \tag{8}$$

where α is the angle of attack between the air stream and the rotor disk (tip-path-plane). The profile power loss (P_{profile}) is given as:

$$P_{\text{profile}} = \frac{\rho A_{\text{rotor}}(\Omega R)^3 \sigma C_{\text{d mean}} F_P}{8}, \tag{9}$$

where Ω is the rotational velocity of the rotor blades, σ is the thrust-to-weight solidity ratio, $C_{\text{d mean}}$ is the mean blade drag coefficient, and F_P is the function that accounts for the increase of the blade section velocity with rotor edgewise and axial speed.

Table 1 Performance data of the eVTOL aircraft [13]

Parameter (Unit)	Value
R (m)	4.0
A_{rotor} (m^2)	50.26
mass (kg)	2,940
σ	0.055
$C_{\text{d mean}}$	0.0089
F_P	0.97
κ	1.75
Ω (rad/sec)	30.12
P_{max} (kw)	494.25

Finally, we can write the instantaneous power required P_{required} in forward flight as:

$$P_{\text{required}} = \kappa \sum_{n=1}^{4}(T_{\text{rotor}})_n(v_i)_n + \frac{\rho A_{\text{rotor}}(\Omega R)^3 \sigma C_{\text{d mean}} F_P}{8} + TV \sin\alpha \tag{10}$$

C. Performance Requirements

The following two mission requirements and path constraints are considered for each flight mission in this paper. First, the net vertical force on the eVTOL aircraft is zero, since we are considering the cruise phase.

$$T \cos\phi \cos\theta = mg \tag{11}$$

Second, the trajectories that the aircraft follow to fly between waypoints are governed by the great-circle trajectory:

$$(V\sin\psi)(\sin\lambda_2\cos\lambda_1 - \sin\lambda_1\cos\lambda_2\cos(\tau_2-\tau_1)) - (V\cos\psi)(\sin(\tau_2-\tau_1)\cos\lambda_2) = 0 \tag{12}$$

D. Energy-optimal Guidance Law Design

Now that we established the power consumption model and performance requirements, we proceed to find the control input trajectories (u_t) that result in an optimal energy consumption. To that end, we formulate the following optimal control problem with an objective function to minimize the mission-level energy consumption, and the performance requirements as constraints.

$$\min_{\forall t\in[0,T_f]} \int_0^{T_f} (P_{\text{required}})\,dt \tag{13}$$

subject to

$$\begin{cases} \dot{x}_t = \xi(x_t, u_t), \\ T\cos\phi\cos\theta - mg = 0, \\ (V\sin\psi)(\sin\lambda_2\cos\lambda_1 - \sin\lambda_1\cos\lambda_2\cos(\tau_2-\tau_1)) \\ \qquad\qquad - (V\cos\psi)(\sin(\tau_2-\tau_1)\cos\lambda_2) = 0 \end{cases} \tag{14}$$

Solving the above optimal control provides optimal energy consumption at a fixed altitude and cruise speed. Hence, to get the optimal energy consumption value for a set of flight plans, the above optimal control problem has to be solved for each flight plan. In this paper, we have used an open-source C++ library called PSOPT [15] to solve the aforementioned nonlinear programming problem numerically using a sparse nonlinear programming solver.

E. Wind Forecast

The energy consumption of eVTOL aircraft is significantly influenced by wind conditions. Specifically, the energy required for the aircraft to counteract the drag forces exerted by the wind must be taken into account to accurately estimate the energy consumption of a flight mission. To that end, a micro-wind service was developed to provide wind forecast information to support the flight planning needs of flight operators and other low-altitude aviation stakeholders. A customized version of the Weather Research and Forecasting (WRF) [16, 17] model was used to generate high-resolution deterministic wind forecasts. The model simulates weather conditions by solving partial differential equations and producing three-dimensional gridded volumes of wind forecasts and other weather products. The model was configured to forecast the Dallas Fort Worth area every 15 minutes at a horizontal resolution of $100m \times 100m$. The forecast data was utilized by a server that could provide forecast wind values at discrete locations when queried over the internet. An application public interface was set up to allow external users to interact with the service by making individual requests for data. Users can specify the points along a four-dimensional trajectory that they intend to fly, and the service will provide them with the weather forecast information to estimate the wind speed and direction at the requested points by interpolating the data at the requested spatial and temporal locations.

IV. Charging Demand Forecasting Procedure

The procedure for forecasting charging demand is illustrated in Figure 1. This process begins by collecting several key inputs specific to the scenario, including the types of aircraft and batteries, a list of flight plans to be executed within the forecast time horizon, and a wind forecast.

A. Feasibility Assessment

The next step in the charging demand forecasting process involves assessing the feasibility of each flight mission using the energy consumption model discussed in Section III.B. This model calculates the energy consumption for each flight plan. This step is crucial because it filters out flight missions that cannot be supported by the maximum battery capacity at the time, due to factors such as strong winds or the length of the flight plan. If a flight mission is deemed infeasible, it is removed from the list of flight plans and either rescheduled to a later time when wind conditions are more favorable or canceled altogether.

Given a set of flight plans $\{F_i\}_{i=1}^{N}$, where N is the total number of flight plans, the feasibility of flight plan F_i is defined as follows:

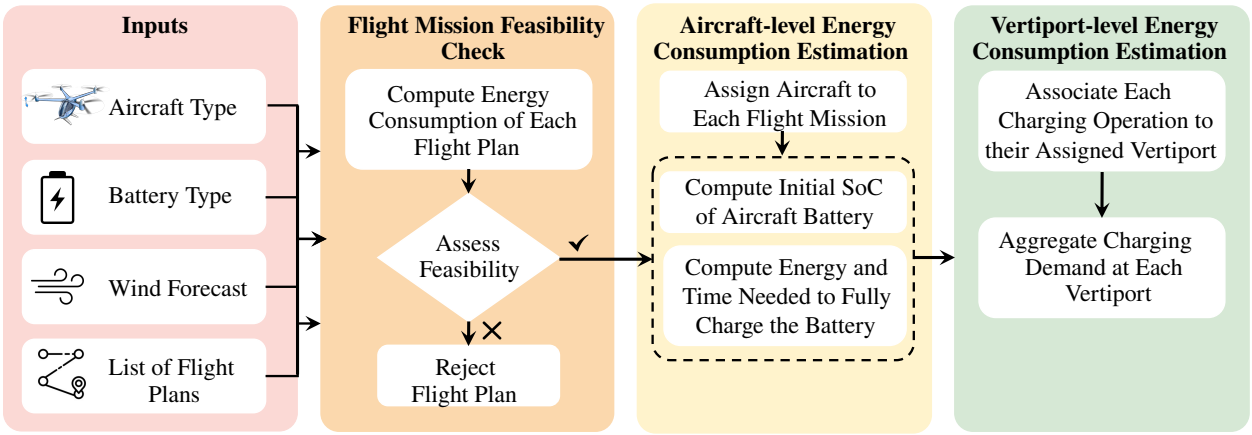

Fig. 1 Charging Demand Forecasting Procedure.

$$\text{Feasibility}(F_i) = \begin{cases} \text{True}, & \text{if } E_{\text{consumed},i} \leq E_{\text{battery}} \\ \text{False}, & \text{if } E_{\text{consumed},i} > E_{\text{battery}} \end{cases} \text{ for } i = 1, 2, \ldots, N \tag{15}$$

where $E_{\text{consumed},i}$ represents the energy consumption of flight plan i, and E_{battery} represents the total battery capacity. In future eVTOL flights, a required amount of contingency energy reserves may be necessary for a flight to be feasible. However, the exact amount required is yet to be determined, so we have neglected it in this paper for simplicity.

B. Computing Charging Demands

After verifying the feasibility of all flight missions, we proceed to compute the charging demands for each aircraft. The initial step in this process involves assigning a set of flight missions to each aircraft in the fleet. For each flight mission assigned to an aircraft, we perform the following operations: first, we compute the initial State of Charge (SoC) of the battery. We assume that before the charging demand forecasting begins, all aircraft in the fleet have an initial SoC between 20% and 30%. Therefore, for all first-flight missions assigned to an aircraft, the initial SoC is randomly assigned within this range. However, for subsequent flights, the SoC of the battery is computed as:

$$\text{SoC}_i = 1 - \frac{E_{\text{consumed},i-1}}{E_{\text{battery}}} \tag{16}$$

Once the SoC is identified, the next step involves computing the energy and time needed to fully charge the battery. This requires a detailed examination of the charging process.

C. Charging Process

The total energy capacity and the charging behavior of the eVTOL battery used in this study are based on [18]. According to [18], a 5-seater Joby S4 eVTOL aircraft has a battery capacity of 160 kWh. The equation representing the charging behavior of a 320 kW charger is given by:

$$P_{\text{charging}}(\text{SoC}) = \begin{cases} P_{\text{charging,max}} & \text{if SoC} \leq 20\% \\ P_{\text{charging,max}} - \gamma * (\text{SoC} - 20) & \text{if SoC} > 20\% \end{cases} \tag{17}$$

where SoC is the initial state of charge percentage of the battery, P_{charging} is the maximum charging power, and γ is the slope of the line. Figures 2 and 3 show the charging process and the time required to fully charge the battery from a given initial state of charge. In addition, given the initial state of charge, the energy needed to fully charge the battery ($E_{\text{full charge}}$) can be computed using:

$$E_{\text{full charge}} = (1 - \text{SoC}) * E_{\text{battery}} \tag{18}$$

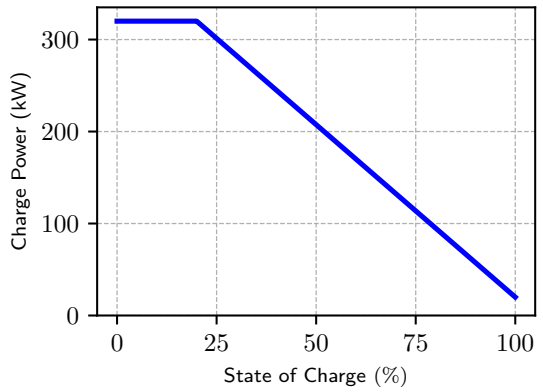

Fig. 2 SoC vs Charging Power of the Charger.

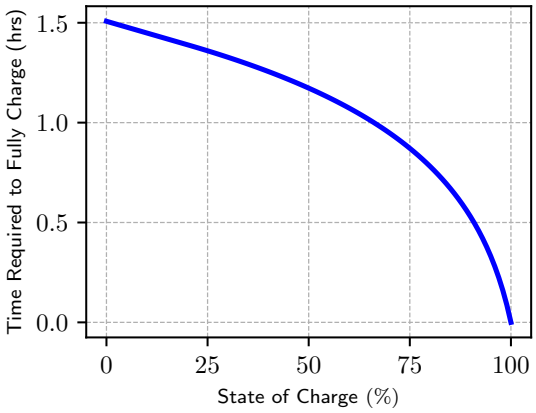

Fig. 3 SoC vs Time to Fully Charge.

D. Aggregating Charging Demands

Once the charging demand of each flight mission for each aircraft is computed, we proceed to forecast the charging demand at the vertiport level. This involves identifying the vertiports where all battery charging operations are conducted for the flight missions. Finally, we aggregate the charging demands at each vertiport for all aircraft, and this aggregated demand represents the total charging demand of the vertiport for the specified time horizon.

V. Results and Discussion

A. Scenario Description

The scenario we adopted in this paper to demonstrate the proposed charging demand forecasting procedure is implemented in the Dallas-Fort Worth (DFW) area, as shown in Figure 4. This scenario includes 112 flight plans and 31 vertiports spread across the entire DFW area. Among these vertiports, 6 are arrival-only vertiports, where all associated aircraft land, and 2 are departure-only vertiports, where all associated aircraft take off. Additionally, there are 23 mixed-use vertiports, accommodating both arriving and departing aircraft. This grouping of vertiports is applicable only for the 4-hour charging load forecasting horizon. As mentioned in Section III.A, all flight missions in this paper are assumed to be cruise flights, with all missions assigned a cruise speed between 50 m/s and 60 m/s at an altitude of 1500 ft AGL. Furthermore, all departing flight missions from a vertiport are scheduled with equal time gaps between each other throughout the entire operational time horizon.

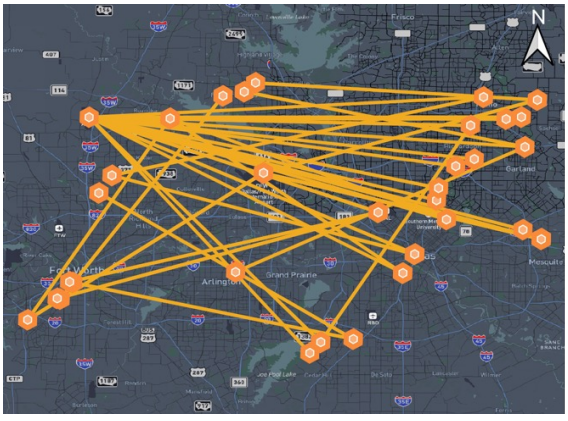

Fig. 4 Implemented Urban Air Mobility Scenario in the DFW Area.

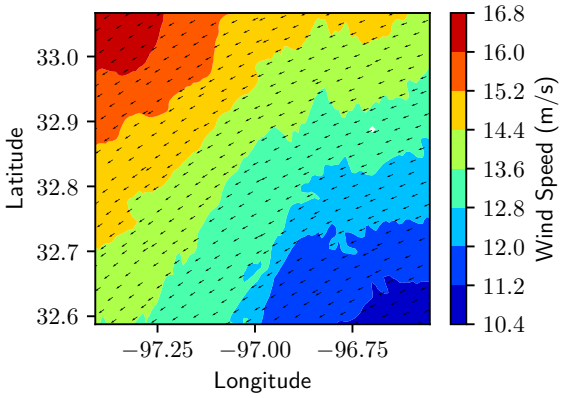

Fig. 5 Wind Forecast at 1:30 PM for the DFW Area.

B. Wind Forecast

The wind forecast data used in this paper is collected for the area shown in Figure 4 for a time frame between 1:30 PM and 5:30 PM on April 20, 2021. Since the flight plans are distributed across this 4-hour period, we collected wind data every 15 minutes. Figure 5 shows an example of the wind forecast data at 1:30 PM at an altitude of 1500 ft. AGL, with the magnitude represented by a heatmap and the wind direction indicated by black arrows.

C. Charging Demand Forecasting

Once the necessary information about the UAM environment is collected, the first step is to check the feasibility of each flight mission in relation to the total battery capacity using Equation 17. In our case, the energy consumption for all 112 flights is below the maximum battery capacity, making them feasible. We then proceed to assign each aircraft in the fleet to the flight missions. With a fleet size of 86 aircraft, most of the aircraft are assigned to one flight mission. Figure 6 shows the aircraft-to-mission assignments, where the x-axis represents the aircraft ID and the y-axis represents the number of missions assigned to each aircraft. As illustrated in the figure, aircraft IDs for those assigned to execute more than one flight mission are shown in separate columns, while the rest are categorized under the *"other"* category.

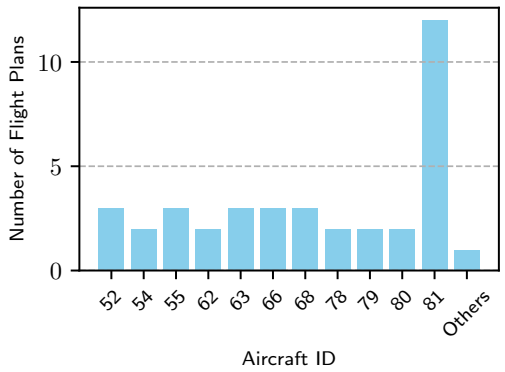

Fig. 6 Aircraft ID vs Number of Flight Plans.

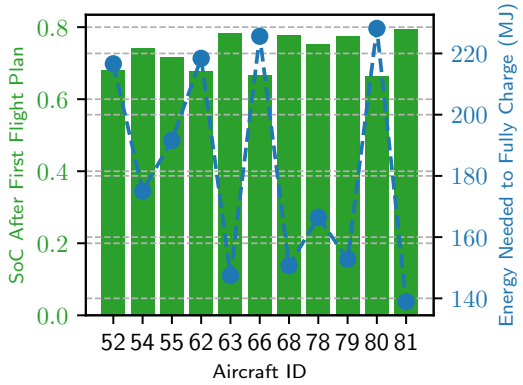

Fig. 7 SoC and Energy Needed to Fully Charge.

After an aircraft is assigned to a flight mission, we compute the initial SoC of the battery before each mission and determine the energy and time needed to fully charge the battery. Figure 7 shows the SoC after the first flight plan for aircraft assigned to perform more than one flight mission, as well as the energy required to fully charge these aircraft batteries to their full capacity. One insight from Figure 7 is that the SoC of most aircraft after completing a flight mission ranges between 60% and 80%. This indicates that the majority of high-energy charging occurs when the aircraft is charged before its first mission. Therefore, implementing a more efficient aircraft routing method is likely to decrease the overall charging demand at the vertiports.

Once the charging energy requirements for all flight missions across all aircraft are calculated, we aggregate these charging demands at all charging vertiports to determine the total charging demand of each vertiport. Figure 8 shows the total energy demand of all 25 charging vertiports in the scenario, as well as the number of flights associated with each vertiport. From the results, it can be observed that as the number of departing flight missions supported by a vertiport increases, the charging demand of that vertiport also increases.

In addition, Figure 9 presents the geographical distribution and relative energy demand of 25 vertiports within the DFW area. Each vertiport is clearly labeled with its ID for easy identification. The color of the markers visually represents the total energy demand at each vertiport, with red indicating higher energy demands and blue indicating lower demands. This visual representation facilitates an understanding of the spatial variation in energy requirements across different locations.

Among the 25 charging vertiports shown in Figures 8 and 9, Vertiport 1, located near Benbrook, TX, has the highest energy demand at 14,319.17 MJ for the 4-hour forecasting horizon. It supports 28 departing flights and is depicted in red. Vertiport 2, situated around Roanoke, TX, follows with an energy demand of 11,673.16 MJ. Additionally, Vertiports 8, 9, and 25, located in the Grapevine, University Park, and Mesquite areas respectively, exhibit relatively higher energy demands compared to the other vertiports in the UAM scenario. Some vertiports, despite having smaller individual energy demands, are located in close proximity to each other. For instance, vertiports around Richardson,

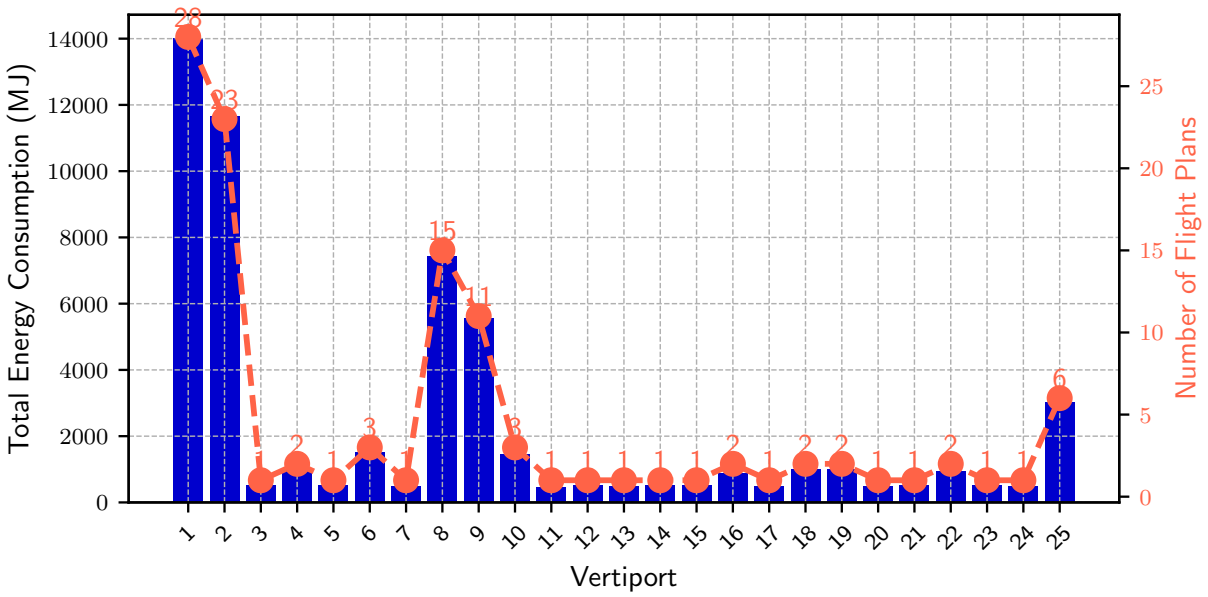

Fig. 8 Total Charging Energy Demand at Each Vertiport and the Number of Flight Plans Associated with Each Vertiport.

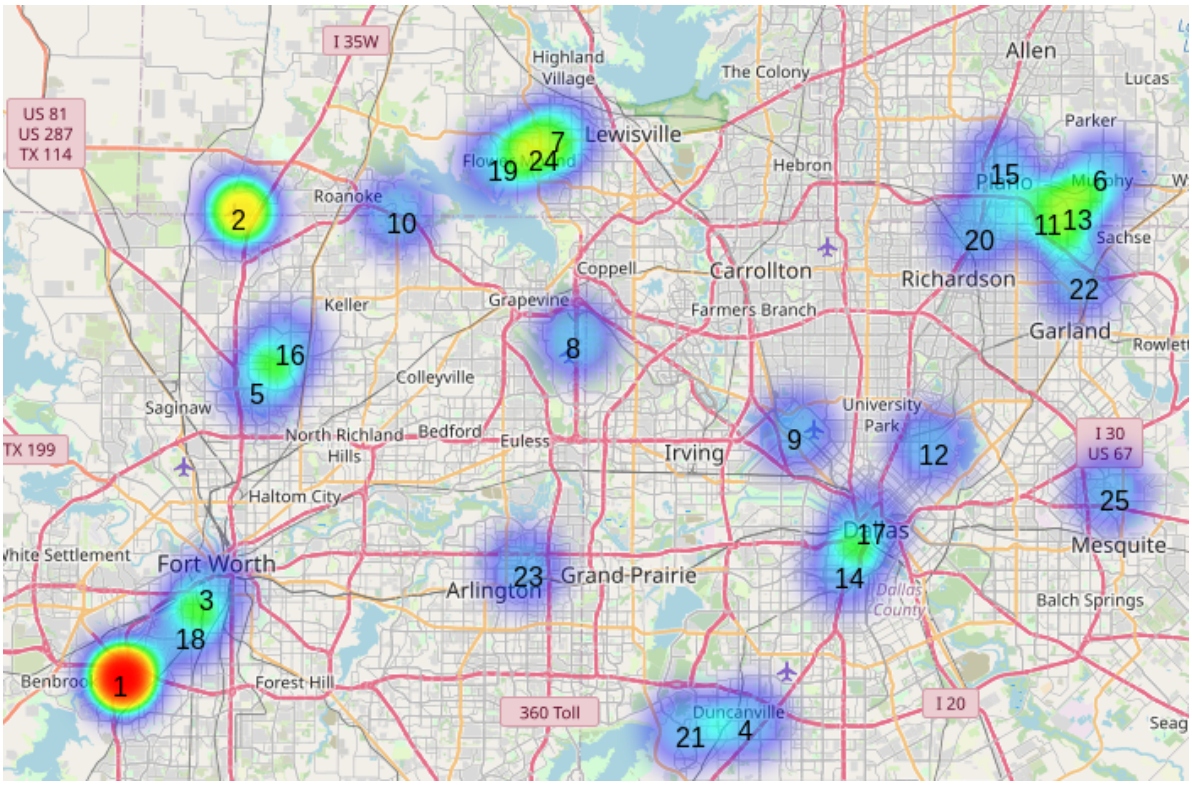

Fig. 9 Location of each charging vertiport on a map. The charging demand for each vertiport over the 4-hour forecasting horizon is depicted using a heat map, with red indicating the highest energy demand and blue indicating the lowest energy demand.

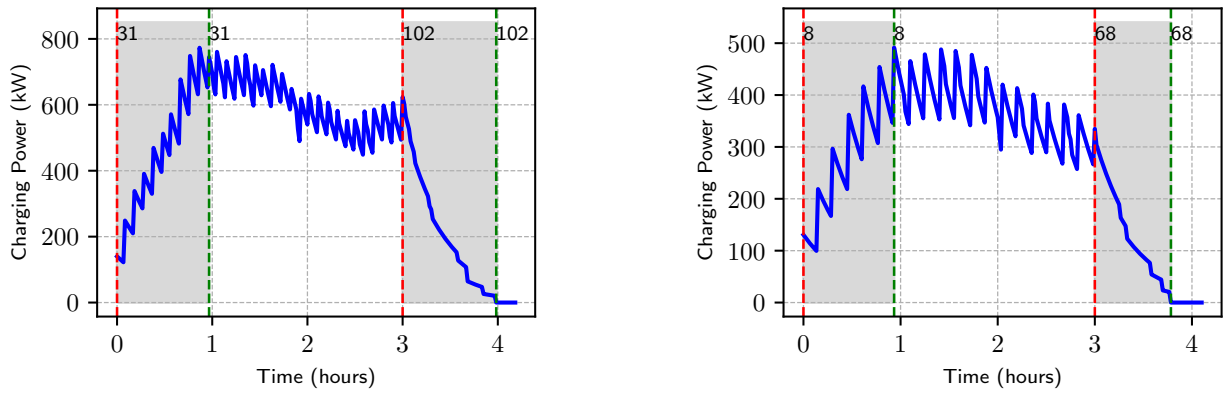

Fig. 10 Charging power profile for Vertiports 1 and 8. Blue lines represent the total charging power. Red dashed lines indicate charging start times, and green dashed lines indicate end times of charging for the first and last flight plans. Shaded gray areas highlight the charging duration for these selected flights, with flight numbers labeled at their respective start and end times.

TX, collectively have a higher energy demand than many other individual vertiports. Strategic planning of the power grid should consider such clusters to ensure efficient and stable electrical energy supply to these areas. These insights are crucial for the effective planning and operation of the power grid serving the charging needs of these vertiports.

Furthermore, Figure 10 shows the charging power demand curves for vertiports 1 and 8 over 4 hours. These plots illustrate the aggregate charging power (in kW) over time (in hours), reflecting the cumulative demand from multiple aircraft charging simultaneously. The blue lines represent the total charging power, oscillating up and down due to the intermittent start and stop of charging events for multiple aircraft. The red dashed lines indicate the start times and the green dashed lines indicate the end times of charging for the first and last flight plans. Shaded gray areas between these lines show the duration of charging for these selected flights, with flight numbers labeled at the start and end times. This visualization highlights how charging demand is distributed temporally, ensuring a balanced load on the vertiport's charging infrastructure. The consistent profile throughout the time horizon, without excessive peaks at the beginning or end, demonstrates a well-distributed arrival and charging schedule for the aircraft.

VI. Conclusion

This study addresses the challenge of forecasting charging demands for urban air mobility (UAM) operations by introducing an energy consumption model-based load forecasting technique. This approach takes into account crucial factors that influence energy consumption in UAM, such as aircraft models, wind forecasts, and detailed flight mission plans. We validated the effectiveness of this framework through a case study involving a large UAM network in the Dallas-Fort Worth (DFW) area, operating within a 4-hour time horizon. In addition, by integrating the charging process with the demand forecasting process, we were able to accurately estimate the aggregated power demand at each vertiport during the forecast period. The findings indicate that the charging demand at a vertiport is significantly impacted by the number of departing flight missions and their departure schedules. The insights gained from this research are relevant for the planning and development of efficient charging infrastructure, ensuring the sustainable and effective implementation of eVTOLs in urban environments.

VII. Acknowledgments

This project is supported by the NASA Grant 80NSSC21M0087 under the NASA System-Wide Safety (SWS) program.

References

[1] Patterson, M. D., Antcliff, K. R., and Kohlman, L. W., "A proposed approach to studying urban air mobility missions including an initial exploration of mission requirements," *Annual Forum and Technology Display*, 2018.

[2] Das, H. S., Rahman, M. M., Li, S., and Tan, C., "Electric vehicles standards, charging infrastructure, and impact on grid integration: A technological review," *Renewable and Sustainable Energy Reviews*, Vol. 120, 2020, p. 109618.

[3] Islam, M. S., Mithulananthan, N., and Hung, D. Q., "A day-ahead forecasting model for probabilistic EV charging loads at business premises," *IEEE transactions on sustainable energy*, Vol. 9, No. 2, 2017, pp. 741–753.

[4] Koyanagi, F., and Uriu, Y., "A strategy of load leveling by charging and discharging time control of electric vehicles," *IEEE Transactions on Power Systems*, Vol. 13, No. 3, 1998, pp. 1179–1184.

[5] Dai, Q., Cai, T., Duan, S., and Zhao, F., "Stochastic modeling and forecasting of load demand for electric bus battery-swap station," *IEEE Transactions on Power Delivery*, Vol. 29, No. 4, 2014, pp. 1909–1917.

[6] Liao, X., Kang, X., Li, M., and Cao, N., "Short term load forecasting and early warning of charging station based on PSO-SVM," *2019 International Conference on Intelligent Transportation, Big Data & Smart City (ICITBS)*, IEEE, 2019, pp. 305–308.

[7] Sun, Q., Liu, J., Rong, X., Zhang, M., Song, X., Bie, Z., and Ni, Z., "Charging load forecasting of electric vehicle charging station based on support vector regression," *2016 IEEE PES Asia-Pacific Power and Energy Engineering Conference (APPEEC)*, IEEE, 2016, pp. 1777–1781.

[8] Dabbaghjamanesh, M., Moeini, A., and Kavousi-Fard, A., "Reinforcement learning-based load forecasting of electric vehicle charging station using Q-learning technique," *IEEE Transactions on Industrial Informatics*, Vol. 17, No. 6, 2020, pp. 4229–4237.

[9] Thipphavong, D. P., "Analysis of Electrical Grid Capacity by Interconnection for Urban Air Mobility," *AIAA Aviation 2022 Forum*, 2022, p. 3316.

[10] Shihab, S. A. M., Wei, P., Shi, J., and Yu, N., "Optimal evtol fleet dispatch for urban air mobility and power grid services," *AIAA Aviation 2020 Forum*, 2020, p. 2906.

[11] Park, W.-J., Song, K.-B., and Park, J.-W., "Impact of electric vehicle penetration-based charging demand on load profile," *Journal of Electrical Engineering & Technology*, Vol. 8, No. 2, 2013, pp. 244–251.

[12] Pradeep, P., Lauderdale, T. A., Chatterji, G. B., Sheth, K., Lai, C. F., Sridhar, B., Edholm, K.-M., and Erzberger, H., "Wind-optimal trajectories for multirotor eVTOL aircraft on UAM missions," *Aiaa Aviation 2020 Forum*, 2020, p. 3271.

[13] Silva, C., Johnson, W. R., Solis, E., Patterson, M. D., and Antcliff, K. R., "VTOL urban air mobility concept vehicles for technology development," *2018 Aviation Technology, Integration, and Operations Conference*, 2018, p. 3847.

[14] Pradeep, P., and Wei, P., "Energy-efficient arrival with rta constraint for multirotor evtol in urban air mobility," *Journal of Aerospace Information Systems*, Vol. 16, No. 7, 2019, pp. 263–277.

[15] Becerra, V. M., "Solving complex optimal control problems at no cost with PSOPT," *2010 IEEE international symposium on computer-aided control system design*, IEEE, 2010, pp. 1391–1396.

[16] Skamarock, W. C., Klemp, J. B., Dudhia, J., Gill, D. O., Liu, Z., Berner, J., Wang, W., Powers, J. G., Duda, M. G., Barker, D. M., and Huang, X. Y., "A description of the advanced research WRF model version 4," Tech. rep., 2019. National Center for Atmospheric Research: Boulder, CO, USA, NCAR/TN-556+STR.

[17] Jones, J. C., Bonin, T., and Mitchell, E., "Evaluating Wind Hazards for Advanced Air Mobility Operations," *AIAA AVIATION 2023 Forum*, 2023, p. 4104.

[18] Burak Onat, E., Bulusu, V., Chakrabarty, A., Hansen, M., Sengupta, R., and Sridar, B., "Evaluating eVTOL Network Performance and Fleet Dynamics through Simulation-Based Analysis," *arXiv e-prints*, 2023, pp. arXiv–2312.